Does the intraperitoneal dexmedetomidine induce bone regeneration in cranial defects at subsedative doses in rabbits?

Gözde Nur Erkan[1], Umut Tekin[1], Özge Boyacıoğlu[2], Petek Korkusuz[3], Kaan Orhan[4], Betül Kırman[1], and Mustafa Ercüment Önder[1]

[1]Kirikkale Universitesi Dis Hekimligi Fakultesi
[2]Hacettepe Universitesi
[3]Hacettepe Universitesi Tip Fakultesi
[4]Ankara Universitesi

April 08, 2024

Abstract

Objective: Dexmedetomidine has been shown to exert protective and curative effects on various tissues and organs in different pathological processes. This study aimed to investigate the effect of dexmedetomidine on the regeneration process after inducing a critical-sized bone defect in the calvarium of rabbits. **Subject and Methods:** Twenty-four male Oryctolagus cuniculus rabbits were divided into three groups, and an 8-mm circular parietal critical-sized bone defect was induced in all groups. Group_LD was given dexmedetomidine 2.75 µg/kg; Group_HD, dexmedetomidine 5.5 µg/kg; and Group_C, saline; all administered intraperitoneally for 7 days. The blood pressure and sedation score of the rabbits were evaluated. Bone tissue samples collected at the end of 8 weeks were examined via micro-computed tomography (micro-CT) and histomorphometry. **Results:** The micro-CT results indicated that regeneration significantly improved in all parameters in the dexmedetomidine-treated groups ($p < 0.001$). Furthermore, low-dose dexmedetomidine statistically significantly increased the bone volume ratio (BV/TV) compared with high-dose dexmedetomidine ($p = 0.002$). Trabecular thickness, connectivity value, and connectivity density were statistically significantly higher in Group_LD than in Group_HD ($p < 0.001$). The highest BA/TA% measurement in histomorphometry was observed in Group_HD, with a mean of $29.81\% \pm 8.52\%$. Significant intramembranous ossification was observed in the dexmedetomidine-treated groups, and active osteoblasts were observed in at the margin of the new bone trabeculae. **Conclusion:** This study demonstrated that dexmedetomidine increases osteoblastic activity and regeneration quality. In particular, low-dose dexmedetomidine exerted a more significant positive effect on the regeneration process and regenerative tissue quality than high-dose dexmedetomidine according to the micro-CT parameters.

Introduction

Regeneration of bone tissue lost due to trauma or an intervention such as cancer surgery is a complex process. Bone repair involves four overlapping phases: initial inflammatory response, soft callus formation, hard callus formation, initial bone fusion, and bone remodelling [1]. Recently, intensive research has been conducted on the improvement of bone healing processes [2–5].

In the literature, there have been studies on bone regeneration that used many different materials, techniques (low-intensity pulsed ultrasound, pulsed electromagnetic fields, dynamic loading, etc.), and pharmacological agents to increase the treatment success rate by improving the quality and resistance of the regenerative tissue [6–13]. On the other hand, gene therapy in rabbits needs to be investigated further to validate the results and test them clinically [4,14].

Dexmedetomidine is a highly selective α2-adrenoceptor agonist with a broad pharmacologic spectrum that

exhibits sedative, anxiolytic, and hypnotic effects in addition to analgesic and sympatholytic properties. The sedative effect is dose-dependent. Low doses induce conscious sedation, whereas higher doses induce deep sedation and general anesthesia [15].

In recent years, the different beneficial effects of dexmedetomidine have been investigated [16–24], and antioxidant, anti-inflammatory, and antiapoptotic effects have been reported [16–19]. The organ-protective and damage-reducing effects of dexmedetomidine against injury in various processes in different tissues and organs have been demonstrated in many studies [20–23]. Most importantly, dexmedetomidine has been shown to increase gene levels related to osteogenesis and angiogenesis as well as reduce apoptosis in osteoporotic rats through the miR-361-5p/VEGFA axis [24]. Another research conducted on fetal osteoblast cell culture reported that dexmedetomidine inhibited apoptosis and increased osteoblastic activity in H2O2-induced oxidative stress model [17]. To the best of our knowledge, there is no study investigating the osteogenic effect of dexmedetomidine on regeneration after the occurrence of critical-sized bone defects.

This study was based on the hypothesis that dexmedetomidine improves bone regeneration after the occurrence of bone defects, especially because the positive effects of dexmedetomidine on the bone tissue were reported in addition to its other beneficial effects. Furthermore, there was no well-defined experimental model for the intraperitoneal (IP) dose of dexmedetomidine in rabbits. Therefore, this study aimed to investigate the beneficial effect of dexmedetomidine on bone regeneration and to establish an experimental model for future studies by determining the hemodynamic side effect and clinical sedation scores that would occur in rabbits at the doses used in this study. Herein, the effects of dexmedetomidine on bone regeneration after the induction of a critical-sized bone defect was investigated radiologically and histomorphometrically.

Materials and Methods

Ethical approval from the Committee on Animal Research and Ethics of Kırıkkale University was obtained for the study (approval number: 2020/08-49). This experimental study conformed to the ARRIVE Guide for the Care and Use of Laboratory Animals [25]. The study was conducted on 24 male, healthy, non-immunocompromised, and non-genetically modified Oryctolagus cuniculus rabbits (20 weeks old and weighing approximately 2.7 kg). The rabbits were kept in separate cages at appropriate light/dark cycle, humidity, and temperature. In addition, they were fed water and standard laboratory chow ad libitum.

1. Experimental Protocol

The rabbits were randomly divided into three groups of eight rabbits each. During the first 7-day inflammatory phase, dexmedetomidine was administered to improve the bone regeneration process.

The organ and tissue protective intraperitoneal dose of dexmedetomidine in rabbits was not clearly identified. It was demonstrated that 1 µg/kg intraperitoneal dexmedetomidine administration had no protective effect on traumatic spinal cord injury in rabbits [26]. However, intravenous dexmedetomidine infusion at a dose of 2.75 µg/kg was shown to be protective against myocardial ischemia-reperfusion injury in rabbits [27]. Intraperitoneal administration of dexmedetomidine at doses of 2.5 and 5 µg/kg has been shown to reduce the severity of vancomycin nephrotoxicity in rats [23]. When the data were evaluated together, it was decided to administer intraperitoneal dexmedetomidine at doses of 2.75 and 5.5 µg/kg and to compare the clinical, radiologic and histomorphometric effects of two different doses.

In the low-dose dexmedetomidine group (Group_LD), the same defect was induced on the rabbits. Dexmedetomidine (Semotidine, 200 µg/2 mL; Vem Pharmaceuticals, Turkey) was initially administered 30 min before the defect induction and then once daily at a dose of 2.75 µg/kg in 5-mL SF at the same time for 7 days.

In the high-dose dexmedetomidine group (Group_HD), the same defect was induced on the rabbits. Dexmedetomidine was initially administered 30 min before the defect induction and then once daily at a dose of 5.5 µg/kg in 5-mL SF at the same time for 7 days.

In the control (Group_C), an 8-mm circular parietal bone defect was induced on the rabbits. Saline (SF, 5

mL) was initially administered 30 min before the defect induction and then once daily at the same time for 7 days.

All injections were administered by the same physician (GNE). Only MEÖ was aware of the group allocation at all stages of the experiment.

General anesthesia was induced by administering 50 mg/kg ketamine HCL (Ketax, 500 mg/10 mL, Vem Pharmaceuticals, Turkey) intramuscularly before surgery. In addition, local anesthesia was induced by administering 2-mL 1/10000 adrenaline-containing articaine HCL (Maxicaine, 80 mg/2 mL+0.01 mg/2 mL, Vem Pharmaceuticals, Turkey) to the skin. After inducing anesthesia, subperiosteal dissection was performed on the left parietal bone. The periosteum was sharply dissected, the flap removed, and the bone tissue exposed. Under saline irrigation, a 2-mm depth was drilled using an 8-mm Trephine Burr. An 8-mm circular bone defect, reported to be the minimum critical bone defect size in the literature [28], was induced by lifting the bone like a cap using an osteotome; the distance between the medial edge of the circular defect and the interparietal suture was 2 mm. The dura mater was protected during the procedure (Figure 1A). After the procedure, the skin and periosteum were closed using 4-0 polyglycolic acid sutures. Furthermore, all rabbits were intramuscularly injected with enrofloxacin 5 mg/kg (Baytril-K 5%, Bayer Healthcare LLC., Turkey) and meloxicam (Meloxicam, 250 mg/50 mL, Bavet Veterinary Pharmaceuticals, Turkey) once daily for 5 days. The rabbits were followed up for 8 weeks. At the end of the 8 weeks after the defect induction, all rabbits were sacrificed via IP administration of a high-dose (150 mg/kg) of pentobarbital (pental sodium, 0.5 g, İ.E. Ulagay, Menarini Group, Turkey). There were no expected or unexpected adverse events in the study. Bone tissue samples were collected to obtain at least 3 mm of intact bone tissue in the region of the defective parietal bone (Figure 1B). The specimens were examined via micro-computed tomography (micro-CT) and histomorphometry.

2. Blood Pressure Measurement and Sedation Scoring

Sedation score and non-invasive blood pressure (NIBP) were determined and measured, respectively, in all rabbits every 5 min within 30 min after IP administration of dexmedetomidine or SF. NIBP measurements were performed using a Mindray uMEC 10 monitor (Shenzhen Mindray Bio-Medical Electronics Co., 2021, China) and a 5–10-cm NIBP cuff. The scoring system used by Raekallio et al. was used here to evaluate sedation (Table 1) [29]. According to the scoring system, 11 was set as the highest sedation score.

3. Micro-Computed Tomography

We used a micro-CT system (Bruker, Skyscan 1275, Belgium) for scanning tissue samples [8]. The structural parameters were tissue volume (TV), bone volume (BV), percent of bone volume (BV/TV ratio), trabecular thickness (TbTh, in millimeters), trabecular spacing (TbSp, in millimeters; mean distance between the trabeculae), connectivity, and connectivity density (ConnDn, 1 per cubic millimeter). These variables were evaluated in three dimensions (3D) as previously done [8].

4. Histomorphometry

The bone samples were fixed in 10% phosphate-buffered formalin (pH 7.0) and decalcified in De Castro solution at room temperature. After rinsing the samples with phosphate buffer and dehydrating in graded ethanol series, they were paraffin-embedded using a vacuum tissue processor (Leica, Germany). Paraffin sections (3–4-µm thick) were prepared using a sliding microtome (Leica, Germany). After staining sections with hematoxylin–eosin (HS) and Masson's trichrome, they were observed under a bright-field microscope (Leica DMB6 B, Wetzlar, Germany) equipped with a digital camera (Leica DFC7000 T, Wetzlar, Germany) to quantitatively evaluate new bone formation in the defect area of the parietal bone. New bone formation was observed on the entire surface of the defect area of each specimen, and the ratio of new bone formation to the total bone surface was quantified using an image processing software (Leica, LAS Germany) as previously done [8,30,31].

5. Statistical Analysis

In the study, the number of rabbits was set so that the power of the test was >80%. The SPSS software (SPSS v25, IBM Statistics, USA) was used for the whole analysis. The independent and dependent variables were expressed as groups and histomorphometry and micro-CT data, respectively. Normal data distribution was evaluated using the Shapiro–Wilk test. Multiple comparisons for the whole raw data of the micro-CT and histomorphometric analyses were conducted using one-way analysis of variance and pairwise comparisons using Tukey's and Duncan's tests. $P < 0.05$ was considered statistically significant. The descriptive statistics of the parametric data were expressed as mean, minimum, and maximum values.

Results

Sedation scores and the NIBP within 30 min after IP dexmedetomidine administration to the rabbits are presented in Table 2. Sedation did not occur in any of the rabbits within 30 min after IP injection, and blood pressure did not change by more than 10%. In all rabbits, blood pressure decreased by less than 10% at the 5th minute compared with that at baseline.

1. Micro-Computed Tomography

The BV/TV ratio, trabecular thickness, trabecular separation, connectivity, and connectivity density were evaluated in the parietal bone tissue in all the groups via in vivo microcomputer scanning (Figure 2). The mean values of the parameters for each group are presented in Table 3.

1.1. Bone Volume Ratio (BV/TV Ratio)

The bone tissues in Group_LD and Group_HD exhibited a statistically significantly higher BV compared with those in Group_C ($p < 0.001$, Figure 3A). Low-dose dexmedetomidine statistically significantly increased the BV/TV ratio compared with high-dose dexmedetomidine ($p = 0.002$).

1.2. Trabecular Thickness

The trabecular thickness in the control was significantly lower than those in the groups treated with high- and low-dose dexmedetomidine ($p < 0.001$, Figure 3B). The trabecular thickness in Group_LD was found to be significantly higher than that in Group_HD ($p < 0.001$, Figure 3B).

1.3. Trabecular Separation

The trabecular separation in the control was significantly higher than that in the groups treated with high- and low-dose dexmedetomidine ($p < 0.001$, Figure 3C). No significant difference was observed between Group_HD and Group_LD when the data were compared via statistical analysis in multiples and pairs (Figure 3C).

1.4. Connectivity

The connectivity values of the bone tissue in the control were statistically significantly lower than those in the groups treated with high- and low-dose dexmedetomidine ($p < 0.001$, Figure 3D). The connectivity value in Group_LD was significantly higher than that in Group_HD ($p < 0.001$, Figure 3D).

1.5. Connectivity Density

The connectivity density in the control was significantly lower than those in the groups treated with high- and low-dose dexmedetomidine ($p < 0.001$, Figure 3E). The connectivity density in Group_LD was significantly higher than that in Group_HD ($p < 0.001$, Figure 3E).

2. Histomorphometry

The defect area did not completely ossify in any of the groups treated with low (Figure 4D, E, F) and high (Figure 4G, H, I) doses of dexmedetomidine and in the control (Fig. 4A, B, C). The highest BA/TA% was observed in Group_HD, with a mean value of 29.81% ± 8.52%. Group_LD and Group_C had mean values of 22.66% ± 5.25% and 25.83% ± 4.81%, respectively. BA/TA% was found to be higher in Group_HD than in Group_C and Group_LD; however, the difference was not significant (Figure 4J). The BA/TA% in Group_LD

was similar to that in Group_C. Intramembranous ossification of the cavity from the periphery and synthesis of the osteoid matrix by osteoblasts within the new bone, characterized by basophilic cementum lines in the sections stained with HS, were observed more clearly in the groups treated with dexmedetomidine than in the control. Active osteoblasts lined up linearly at the edges of the new bone trabeculae. In the sections triple-stained with Masson's trichrome, the new bone in the calcification process was stained green and the mature bone red.

Discussion This study demonstrated that dexmedetomidine increased the quality and quantity of bone formation measured via micro-CT and histomorphometry at subsedative doses when used for a critical-sized bone defect for an 8-weeks' time period. In the histomorphometric evaluation, it was noteworthy that intramembranous ossification and osteoblast activation were observed in the dexmedetomidine-treated groups. Dexmedetomidine was approved by the Food and Drug Administration in 1999. It can be used as an anesthetic or sedative for patients who are intubated and mechanically ventilated in the intensive care unit as well as in patients who are not intubated during procedural sedation [32].

This study investigated the effects of intraperitoneally administered dexmedetomidine on critical-sized cranial bone defect regeneration, systemic hemodynamics, and sedation score at doses of 2.75 and 5.5 μg/kg. Our results indicated no significant change in blood pressure at the aforementioned doses. Dexmedetomidine intravenously administered at doses of 2.75 and 5.5 μg/kg did not seriously affect hemodynamic parameters [33]. On the contrary, intravenous infusion of dexmedetomidine at a dose of 2.75 μg/kg reduced the magnitude of myocardial ischemia and protected the myocardium from ischemia reperfusion injury [27]. However, an IP dose of 1 μg/kg did not exert beneficial effect in traumatic spinal cord injury [26]. Our results on the unchanged blood pressure were in agreement with those of the previous literature at the 5th minute. The high blood pressure measurements immediately after IP injection may be due to stress. In a study conducted on rabbits, the mean sedation score after intramuscular injection of 25 μg/kg dexmedetomidine and 0.2 mg/kg midazolam was reported to be 10.0 [29,34]. According to the same scoring system, the score was 0 in all rabbits in Group_LD and Group_C, whereas some rabbits in Group_HD were sitting with their heads up and thus scored 1. In this regard, it has been demonstrated that sedation did not occur in any of the rabbits at the doses used in this study. Consequently, an experimental model in which dexmedetomidine could be intraperitoneally administered to rabbits at doses of 2.75 and 5.5 μg/kg without causing clinical sedation and hemodynamic change could be used in various experimental studies.

Our study revealed that dexmedetomidine significantly increased the BV/TV ratio, trabecular thickness and density, connectivity, and connectivity density by micro-CT in Group_LD and Group_HD on week 8 compared with the control. Low-dose dexmedetomidine (2.75 μg/kg) improved all of the micro-CT parameters of ossification better than those of high-dose dexmedetomidine (5.5 μg/kg). Dexmedetomidine was also found to increase BA/TA% by histomorphometry in Group_HD compared with the control and Group_LD, with no statistical significance. Few studies have reported evidence of the beneficial effects of dexmedetomidine on human fetal osteoblasts and osteoporotic rats (17,24). Yoon and colleagues demonstrated that 5 μM dexmedetomidine pretreatment in human fetal osteoblast cell line in an H2O2-induced oxidative stress model increased cell viability by MTT assay, inhibited apoptosis by Annexin-V FITC/PI staining and increased osteoblastic activity by bone nodular mineralization using Alizarin red S staining [17]. Our study did not evaluate the in vitro performance of dexmedetomidine at the cellular level because the research question was based on the healing capacity of the critical-sized cranial defect animal model. Our in vivo model demonstrated an improved ossification parallel to the increased osteoblastic activity in the previous in vitro study but by systemic administration of the same medicine at different doses at different time points.

The osteogenesis- and angiogenesis-triggering effects of dexmedetomidine were demonstrated in a rat ovariectomy-induced osteoporosis model when administered at a dose of 20 μg/kg into the knee at 8 weeks following ovariectomy via micro-CT, HE staining, and western blot analysis [24]. Dexmedetomidine was found to increase the BV/TV ratio, bone mineral density, and trabecular thickness and decreased trabecular separation via micro-CT in rat femur. Furthermore, it increased the expressions of angiogenesis-related (VEGFA and PDGF) and osteogenesis-related (BMP-2, OPG, and Runx2) genes by inhibiting miR-361-5p

via western blot. Improvement of the osteoporosis degree was demonstrated in HE staining by histopathological assessment [24]. In the present study, dexmedetomidine, when administered intraperitoneally 30 min before the critical-sized bone defect surgery, significantly increased the BV/TV ratio, trabecular thickness, connectivity, and connectivity density and significantly decreased trabecular separation by micro-CT. Intramembranous ossification and synthesis of osteoid matrix by osteoblasts within the new bone were observed more clearly in the dexmedetomidine-treated groups compared with the control in HE staining by histopathological assessment.

During the initial 7-day inflammatory phase, the negative effects of prolonged and increased release of inflammatory cytokines (TNF-α, TGF-β, IL1-β, IL6, IL18, and IL23) on the bone are well known [35]. However, a short-term and controlled inflammatory response is critical for bone healing [34]. The anti-inflammatory effect of dexmedetomidine has been demonstrated in various studies [36,37]. It was considered that dexmedetomidine administered during the inflammatory phase may have improved regeneration quality by controlling excessive inflammatory response in our study. The micro-CT findings indicated that the regeneration quality was slightly lower in Group_HD than in Group_LD. Although the inflammatory mediators were not studied, it was thought that dexmedetomidine administered at a dose of 5.5 μg/kg significantly suppressed the inflammatory response, limiting the effect of increased regeneration quality. Our study also demonstrated increased new bone formation by micro-CT and histomorphometry within the critical-sized cranial defect area on week 8 following repeated IP injections.

In this study, dexmedetomidine significantly increased the BV/TV ratio by micro-CT and the BA/TA ratio by histomorphometry, with no statistical significance. A study that compared micro-CT and histomorphometric evaluations reported that due to the processing technique, tissue shrinkage may occur during fixation, dehydration, and clearing, which would affect the digital histomorphometric measurements, so that micro-CT evaluation can provide more accurate information compared with histomorphometry [38]. Bone formation is a 3D process; therefore, techniques that provide 3D images are preferred for evaluation rather than those that provide 2D images, such as histologic micrographs [30]. Studies conducted on different tissues have shown very different levels of correlation between the results of micro-CT and histomorphometry [30,39,40]. Thus, correlation between different parameters could not always be demonstrated on a limited number of rabbits due to ethical regulations and the single time frame.

This study investigated whether dexmedetomidine had a positive or negative effect on the healing process after the induction of bone defect. Therefore, the lack of research into the mechanisms underlying the healing effect of dexmedetomidine is likely to be a limitation of our study. Furthermore, heart rate and peripheral oxygen saturation could not be evaluated for the hemodynamic effects because the rabbits were not sedated or immobilized.

Conclusion

This study demonstrated the beneficial effect of dexmedetomidine on bone regeneration on a critical-sized cranial defect model. It became clear that further experimental studies, including studies on the dose and pathophysiological mechanism, need to be planned to substantiate the beneficial effect of dexmedetomidine on bone regeneration. In this regard, the results of the study were expected to lead to the conduct of experimental and clinical studies in the future.

A cknowledgement

Thanks for the funding provided by Scientific Research Projects Coordination Unit of Kırıkkale University.

Ethics approval statement

Approval numbered 2020/08-49 was obtained from the Committee on Animal Research and Ethics of Kırıkkale University for the study.

Conflict of Interest Statement

The authors declare that they have no conflicts of interest.

Funding Sources

This work was supported by Scientific Research Projects Coordination Unit of Kırıkkale University. Project number; 2020/08-49.

Author Contributions

GNE, MEÖ, UT: Study design; GNE, MEÖ, UT, BK: Implementation of the experimental protocol, GNE, BK: Analysis of clinical data of rabbits, PK, KO, ÖB: Analysis of histomorphometrical and radiological data, GNE: Data collection and writing up of the first draft of the paper, MEÖ, UT, PK, KO: Review of the article text.

Data Availability Statement

The data that support the findings of this study are available from the corresponding author upon reasonable request.

References

1. Schindeler A, McDonald MM, Bokko P, Little DG. Bone remodeling during fracture repair: The cellular picture. Semin Cell Dev Biol. 2008;19(5):459-466. doi:10.1016/J.SEMCDB.2008.07.004

2. Stafford PR, Norris BL. Reamer-irrigator-aspirator bone graft and bi Masquelet technique for segmental bone defect nonunions: a review of 25 cases. Injury. 2010;41 Suppl 2(SUPPL. 2). doi:10.1016/S0020-1383(10)70014-0

3. Henrich D, Seebach C, Sterlepper E, Tauchmann C, Marzi I, Frank J. RIA reamings and hip aspirate: a comparative evaluation of osteoprogenitor and endothelial progenitor cells. Injury. 2010;41 Suppl 2(SUPPL. 2). doi:10.1016/S0020-1383(10)70012-7

4. Giannoudis P V., Jones E, Einhorn TA. Fracture healing and bone repair. Injury. 2011;42(6):549-550. doi:10.1016/J.INJURY.2011.03.037

5. Ghimire S, Miramini S, Richardson M, Mendis P, Zhang L. Role of Dynamic Loading on Early Stage of Bone Fracture Healing. Ann Biomed Eng. 2018;46(11):1768-1784. doi:10.1007/S10439-018-2083-X

6. Wang X, Tong S, Huang S, Ma L, Liu Z, Zhang D. Application of a New Type of Natural Calcined Bone Repair Material Combined with Concentrated Growth Factors in Bone Regeneration in Rabbit Critical-Sized Calvarial Defect. Biomed Res Int. 2020;2020. doi:10.1155/2020/8810747

7. Gao R, Watson M, Callon KE, et al. Local application of lactoferrin promotes bone regeneration in a rat critical-sized calvarial defect model as demonstrated by micro-CT and histological analysis. J Tissue Eng Regen Med. 2018;12(1):e620-e626. doi:10.1002/term.2348

8. Altay B, Dede EÇ, Özgul Ö, et al. Effect of Systemic Oxytocin Administration on New Bone Formation and Distraction Rate in Rabbit Mandible. J Oral Maxillofac Surg. 2020;78(7):1171-1182. doi:10.1016/j.joms.2020.03.005

9. Alp YE, Taskaldiran A, Onder ME, et al. Effects of Local Low-Dose Alendronate Injections Into the Distraction Gap on New Bone Formation and Distraction Rate on Distraction Osteogenesis. J Craniofac Surg. 2017;28(8):2174-2178. doi:10.1097/SCS.0000000000002615

10. Giannoudis P V., Suk M, Pape HC. RIA: The journey just started but what the future holds? Injury. 2010;41 Suppl 2(SUPPL. 2):S1. doi:10.1016/S0020-1383(10)00812-0

11. Cobbs KF. RIA use in a community orthopedic trauma practice: applying technology, respecting biology. Injury. 2010;41 Suppl 2(SUPPL. 2). doi:10.1016/S0020-1383(10)70015-2

12. Busse JW, Bhandari M, Kulkarni A V., Tunks E. The effect of low-intensity pulsed ultrasound therapy on time to fracture healing: a meta-analysis. CMAJ. 2002;166(4):437-441. Accessed April 20, 2022.

https://pubmed.ncbi.nlm.nih.gov/11873920/

13. Fischer V, Haffner-Luntzer M, Amling M, Ignatius A. Calcium and vitamin D in bone fracture healing and post-traumatic bone turnover. Eur Cell Mater. 2018;35:365-385. doi:10.22203/ECM.V035A25

14. Tang Y, Tang W, Lin Y, et al. Combination of bone tissue engineering and BMP-2 gene transfection promotes bone healing in osteoporotic rats. Cell Biol Int. 2008;32(9):1150-1157. doi:10.1016/j.cellbi.2008.06.005

15. Yuen VMY. Dexmedetomidine: perioperative applications in children. Paediatr Anaesth. 2010;20(3):256-264. doi:10.1111/J.1460-9592.2009.03207.X

16. Bao N, Tang B. Organ-Protective Effects and the Underlying Mechanism of Dexmedetomidine. Mediators Inflamm. 2020;2020. doi:10.1155/2020/6136105

17. Yoon JY, Park JH, Kim EJ, et al. Dexmedetomidine attenuates H2O2-induced cell death in human osteoblasts. J Dent Anesth Pain Med. 2016;16(4):295-302. doi:10.17245/jdapm.2016.16.4.295

18. Qiao H, Sanders RD, Ma D, Wu X, Maze M. Sedation improves early outcome in severely septic Sprague Dawley rats. Crit Care. 2009;13(4). doi:10.1186/CC8012

19. Yeh YC, Wu CY, Cheng YJ, et al. Effects of Dexmedetomidine on Intestinal Microcirculation and Intestinal Epithelial Barrier in Endotoxemic Rats. Anesthesiology. 2016;125(2):355-367. doi:10.1097/ALN.0000000000001135

20. Peng K, Chen WR, Xia F, et al. Dexmedetomidine post-treatment attenuates cardiac ischaemia/reperfusion injury by inhibiting apoptosis through HIF-1α signalling. J Cell Mol Med. 2020;24(1):850-861. doi:10.1111/jcmm.14795

21. Cheng J, Zhu P, Qin H, et al. Dexmedetomidine attenuates cerebral ischemia/reperfusion injury in neonatal rats by inhibiting TLR4 signaling. J Int Med Res. 2018;46(7):2925-2932. doi:10.1177/0300060518781382

22. Liang S, Wang Y, Liu Y. Dexmedetomidine alleviates lung ischemia-reperfusion injury in rats by activating PI3K/Akt pathway. Eur Rev Med Pharmacol Sci. 2019;23(1):370-377. doi:10.26355/EURREV_201901_16785

23. Bayram A, Erkan GN, Talih G, et al. The alpha-2 receptor agonist dexmedetomidine attenuates vancomycin-induced acute kidney injury. Bratisl Lek Listy. 2019;120(6):429-433. doi:10.4149/BLL_2019_069

24. Wang Z, Ge X, Wang Y, Liang Y, Shi H, Zhao T. Mechanism of dexmedetomidine regulating osteogenesis-angiogenesis coupling through the miR-361-5p/VEGFA axis in postmenopausal osteoporosis. Life Sci. 2021;275. doi:10.1016/J.LFS.2021.119273

25. Percie du Sert N, Hurst V, Ahluwalia A, et al. The ARRIVE guidelines 2.0: Updated guidelines for reporting animal research. PLoS Biol. 2020;18(7):e3000410. Published 2020 Jul 14. doi:10.1371/journal.pbio.3000410

26. Aslan A, Cemek M, Eser O, et al. Does dexmedetomidine reduce secondary damage after spinal cord injury? An experimental study. Eur Spine J. 2009;18(3):336-344. doi:10.1007/s00586-008-0872-x

27. Ren J, Li C, Liu Y, Liu H, Dong Z. Protective effect of dexmedetomidine against myocardial ischemia-reperfusion injury in rabbits. Acta Cir Bras. 2018;33(1):22-30. doi:10.1590/S0102-865020180010000003

28. Delgado-Ruiz RA, Calvo-Guirado JL, Romanos GE. Critical size defects for bone regeneration experiments in rabbit calvariae: systematic review and quality evaluation using ARRIVE guidelines. Clin Oral Implants Res. 2015;26(8):915-930. doi:10.1111/CLR.12406

29. Raekallio M, Ansah OB, Kuusela E, Vainio O. Some factors influencing the level of clinical sedation induced by medetomidine in rabbits. J Vet Pharmacol Ther. 2002;25(1):39-42. doi:10.1046/J.1365-2885.2002.00382.X

30. Yeom HR, Blanchard S, Kim S, Zunt S, Chu TMG. Correlation between micro-computed tomography and histomorphometry for assessment of new bone formation in a calvarial experimental model. J Craniofac Surg. 2008;19(2):446-452. doi:10.1097/SCS.0B013E318052FE05

31. Aroni MAT, de Oliveira GJPL, Spolidório LC, et al. Loading deproteinized bovine bone with strontium enhances bone regeneration in rat calvarial critical size defects. Clin Oral Investig. 2019;23(4):1605-1614. doi:10.1007/s00784-018-2588-6

32. Pollock M, Wong J. Pediatric Postmarketing Pharmacovigilance and Drug Utilization Review Drug Use Analyst. Published online 2016.

33. Ren J, Li C, Ma S, Wu J, Yang Y. Impact of dexmedetomidine on hemodynamics in rabbits. Acta Cir Bras. 2018;33(4):314-323. doi:10.1590/S0102-865020180040000003

34. Bellini L, Banzato T, Contiero B, Zotti A. Evaluation of sedation and clinical effects of midazolam with ketamine or dexmedetomidine in pet rabbits. Vet Rec. 2014;175(15):372. doi:10.1136/VR.102595

35. Valparaiso AP, Vicente DA, Bograd BA, Elster EA, Davis TA. Modeling acute traumatic injury. J Surg Res. 2015;194(1):220-232. doi:10.1016/J.JSS.2014.10.025

36. Qiu Z, Lu P, Wang K, et al. Dexmedetomidine Inhibits Neuroinflammation by Altering Microglial M1/M2 Polarization Through MAPK/ERK Pathway. Neurochem Res. 2020;45(2):345-353. doi:10.1007/s11064-019-02922-1

37. Zhang J, Wang Z, Wang Y, Zhou G, Li H. The effect of dexmedetomidine on inflammatory response of septic rats. BMC Anesthesiol. 2015;15(1). doi:10.1186/S12871-015-0042-8

38. Boca C, Truyen B, Henin L, et al. Comparison of micro-CT imaging and histology for approximal caries detection. Sci Rep. 2017;7(1):6680. Published 2017 Jul 27. doi:10.1038/s41598-017-06735-6

39. Rüegsegger P, Koller B, Müller R. A microtomographic system for the nondestructive evaluation of bone architecture. Calcif Tissue Int. 1996;58(1):24-29. doi:10.1007/BF02509542

40. Müller R, Van Campenhout H, Van Damme B, et al. Morphometric analysis of human bone biopsies: a quantitative structural comparison of histological sections and micro-computed tomography. Bone. 1998;23(1):59-66. doi:10.1016/s8756-3282(98)00068-4

Table Legends

Table 1. Semi-quantitative sedation level assessment scale in rabbits [29].

Table 2. Non-invasive blood pressure (NIBP) and sedation score assessment results.

Table 3. Evaluation of micro-CT parameters.

Figure Legends

Figure 1. *A:* Implementation of circular bone defect surgery. *B:* Collection of bone tissue samples after sacrification. X: Margin of the circular bone defect area.

Figure 2. 3D micro-CT images. *Group a:* Low-dose dexmedetomidin application there is a considerable amount of new bone formation showing on micro-CT images. *Group b:* High-dose dexmedetomidin application, there is bone healing but less than previous group. *Group c:* Control group showing defective bone areas without healing on micro-CT images.

Figure 3. In bone tissues of the control group (Group_C) and high- (Group_HD) and low-dose (Group LD) dexmedetomidine applied groups by *in vivo* microcomputer scanning (A) bone volume/total volume (BV/TV), (B) trabecular thickness, (C) trabecular separation, (D) connectivity, and (E) connectivity density are given as mean-standard deviation graph. Accordingly, a: control, b: high-dose dexmedetomidine and c: low-dose dexmedetomidine indicate a statistically significant difference ($p < 0.05$).

Figure 4. Left column (*A, D, G*) depicts the low-magnified tile scan images used to measure the defect area (DA) and new bone (NB) area (*40x*). Middle column shows the new bone formation at the edge of the defect area at high magnification (*B, E, H*). Osteoid (Os) is observed in green, and new bone trabeculae in the calcification process in green to red with Masson's Trichrome (MT) (*100x*). In the right column (*C, F, I*), osteoblasts (Ob), cement lines (C), and osteocytes (O) located in the lacunae were observed in the region where the osteoid is replaced by calcified bone in the defect area (*400x*). Group_C: Control; Group_LD: Low-dose dexmedetomidine-applied group; Group_HD: High-dose dexmedetomidine-applied group; MT: Masson's Trichrome; HE: Hematoxylin-eosin. The mean-standard deviation plot (*J*) shows the histomorphometric analysis results. The ratio of the newly-formed bone surface area in the defect area to the total bone surface area BA/TA(%) was measured.

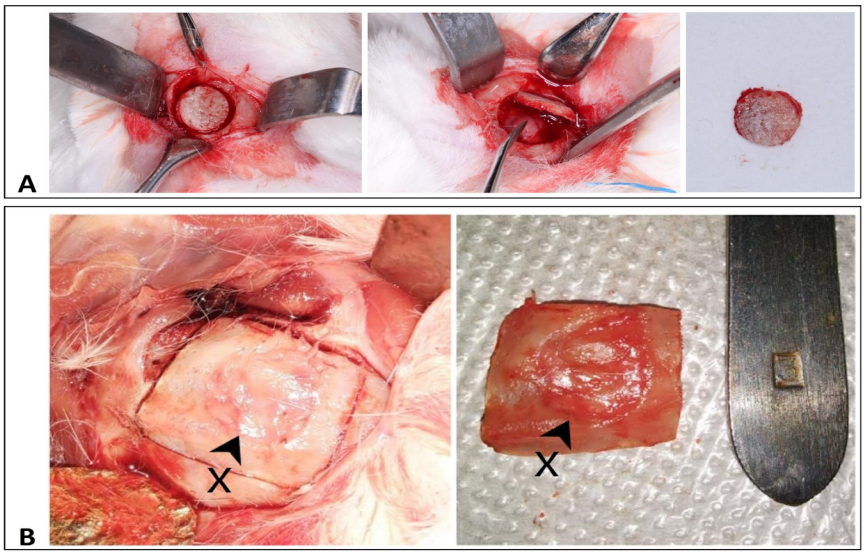

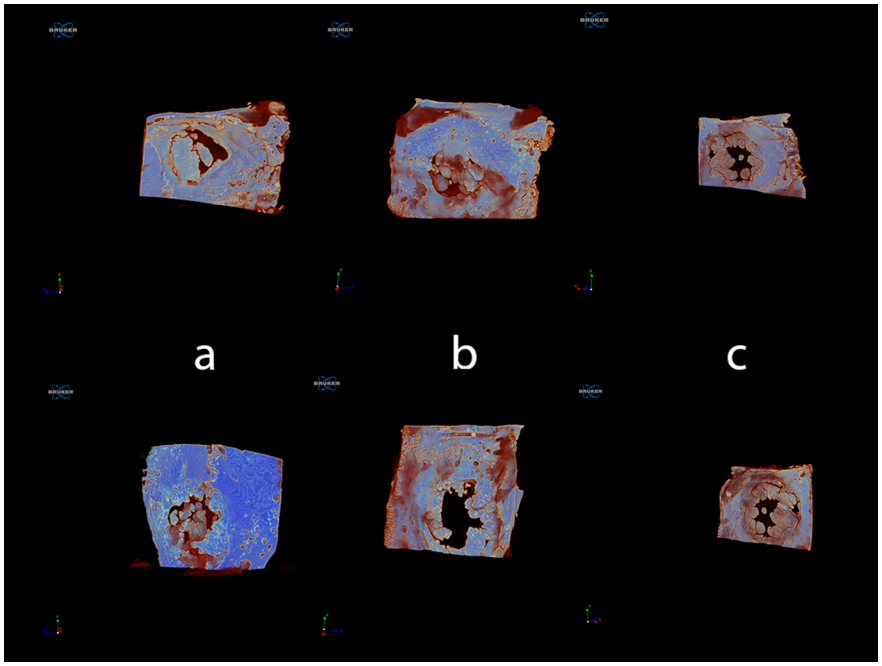

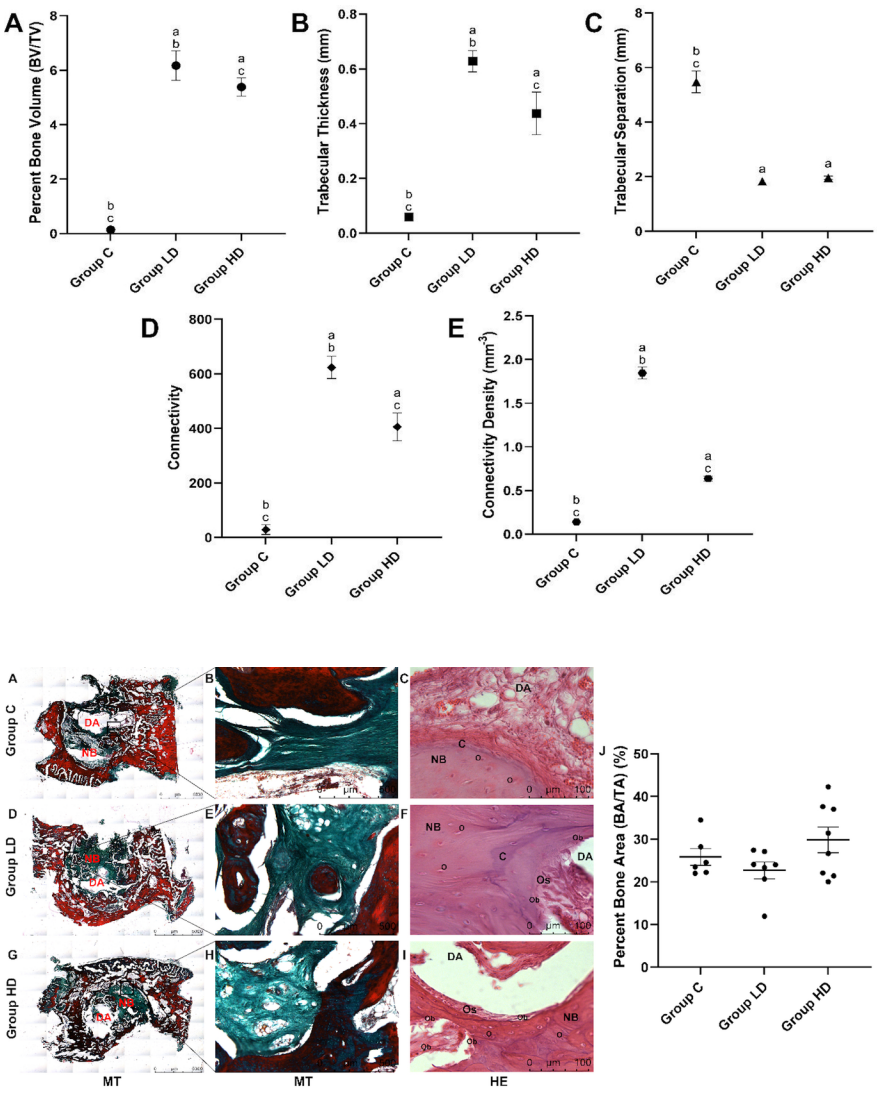

Hosted file

TABLES.docx available at https://authorea.com/users/765281/articles/774086-does-the-intraperitoneal-dexmedetomidine-induce-bone-regeneration-in-cranial-defects-at-subsedative-doses-in-rabbits